Colloids and Surfaces B: Biointerfaces 149 (2017) 312–321

Contents lists available at ScienceDirect

Colloids and Surfaces B: Biointerfaces

journal homepage: www.elsevier.com/locate/colsurfb

Real-time label-free detection and kinetic analysis of Etanercept—Protein A interactions using quartz crystal microbalance

Evan A. Dubiel[a,b], Bruno Martin[a], Sylvain Vigier[a,b], Patrick Vermette[a,b,*]

[a] Laboratoire de bio-ingénierie et de biophysique de l'Université de Sherbrooke, Department of Chemical and Biotechnological Engineering, Université de Sherbrooke, 2500, boulevard de l'Université, Sherbrooke, Québec J1K 2R1, Canada
[b] Research Centre on Aging, Institut universitaire de gériatrie de Sherbrooke, 1036, rue Belvédère Sud, Sherbrooke, Québec J1H 4C4, Canada

ARTICLE INFO

Article history:
Received 19 April 2016
Received in revised form 5 October 2016
Accepted 19 October 2016
Available online 19 October 2016

Keywords:
Quartz crystal microbalance (QCM)
Ligand-receptor interactions
Biologics
Interaction kinetics
Biosensors
Biopharmaceuticals

ABSTRACT

A quartz crystal microbalance (QCM) was constructed to assess if such a biosensor has value as a complementary real-time label-free analysis platform for the biopharmaceutical industry. This was achieved through modifying QCM crystals with a low-fouling carboxymethyl-dextran layer bearing Protein A, and then injecting solutions containing Etanercept (*i.e.*, Enbrel®) into the QCM chambers. The kinetics of Enbrel® – Protein A interactions was modeled using the Langmuir binding model and Enbrel® concentrations between 0.75–300 ng mL^{-1}. The resulting equilibrium dissociation and association constants (K_D and K_A) were 5.06×10^{-8} M and 1.98×10^{7} M^{-1}, respectively. The association and dissociation rate constants (k_{on} and k_{off}) decreased substantially as Enbrel® concentration, *[C]*, increased, despite that the net binding rate, ($k_{on}[C] + k_{off}$), increased. The decrease in k_{on} and k_{off} was hypothesized to be a consequence of mass transport limitations. To verify this, QCM dissipation measurements were analyzed to provide insight on solution viscosity. As Enbrel® concentration increased, the net change in dissipation, ΔD, became larger. An augmentation of ΔD is associated with a higher solution viscosity, which would result in an increase in mass transport limitations. Therefore, the decrease in k_{on} and k_{off} for increasing Enbrel® concentration can be attributed to mass transport limitations. In conclusion, QCM is a valuable complementary real-time label-free biosensor analysis platform for the biopharmaceutical industry. Unlike the surface plasmon resonance (SPR) platform, QCM allows measuring dissipation, which can provide insight on how mass transport limitations impact interaction kinetics.

1. Introduction

Biosensor assays with real-time and label-free attributes have found use in multiple areas of biopharmaceutical research, development, and production through their ability to assess the kinetics of ligand – receptor interactions. A common application of these assays is assessing the binding affinities of therapeutic biologics to their target molecules [1]. Such assays are also used to evaluate the immunogenicity of biologics [2,3]. In addition, these assays have found use for analyzing protein interactions to develop and optimize effective methods for antibody purification [4]. With such an assay, manufacturing processes can be monitored to measure the quantity of antibodies or proteins produced and their associated bioactivity [5,6].

The most common real-time and label-free biosensor assay used in the biopharmaceutical industry is surface plasmon resonance (SPR) [7]. While SPR has been successfully utilized in each of the aforementioned applications, the technique is not without pitfalls. An intrinsic drawback is that SPR measurements provide no insight on the viscosity of the solution being injected over the biosensor surface. As solution viscosity increases, mass transport limitations become more impactful on measured kinetics. For example, in SPR platforms, because of mass transport limitations, the real kinetic rate and equilibrium constants could be up to two to three magnitudes greater than those observed from other measurements [8].

Quartz Crystal Microbalance (QCM) with dissipation measurements is another real-time label-free biosensor method. QCM has been used to monitor ligand – receptor interaction kinetics [9–12], but to a far lesser extent compared to SPR. An intrinsic feature of QCM that appears to be overlooked in previous kinetic studies is dissipation measurements. Dissipation measurements in QCM, defined as the "half-bandwidth at half maximum" of the resonance curve divided by the maximum frequency of the resonance

* Corresponding author at: Department of Chemical and Biotechnological Engineering, Université de Sherbrooke, 2500, boul. de l'Université Sherbrooke, Québec J1K 2R1, Canada.
E-mail address: Patrick.Vermette@USherbrooke.ca (P. Vermette).

http://dx.doi.org/10.1016/j.colsurfb.2016.10.036
0927-7765/

curve, give valuable information regarding the viscosity of the solution and the viscoelasticity of the film [13]. As already mentioned, solution viscosity can greatly impact kinetic rate and equilibrium constants calculated from SPR data. Thus, unlike SPR, QCM can provide valuable insight regarding the effects of solution viscosity on the calculated kinetic rate and equilibrium constants. In this study, we use both QCM frequency to assess ligand – receptor interaction kinetics and dissipation measurements to hypothesize the effects mass transport limitations play on the observed kinetic rate constants.

In this study, a QCM instrument was designed and constructed in-house to study interactions between Protein A and Etanercept. This is also the first study we are aware of to assess interaction kinetics between Protein A and Etanercept. Protein A was immobilized onto QCM crystals and Etanercept solutions of various concentrations were exposed to the modified crystals. Protein A is a cell-wall protein containing five high-affinity binding sites capable of interacting with the F_c-portion of various IgG antibodies. Protein A was chosen for this study as when immobilized on surfaces, it can be used for the purification of therapeutic antibodies [14] as well as to monitor and optimize bioprocesses (when employing Biacore's commercially available Protein A-modified SPR sensors). Etanercept (known by its tradename as Enbrel®) is a biologic that acts as an antagonist towards tumor necrosis factor (TNF). TNF is a soluble inflammatory cytokine that regulates immune cell signaling. TNF dysregulation is associated with numerous inflammatory diseases such as rheumatoid arthritis, Crohn's, and psoriasis to name a few [15]. Enbrel® was chosen for this study as it is currently used extensively to treat many TNF-associated diseases. Biologics like Enbrel® are very costly. Optimizing and understanding downstream processing of biologics is of importance for the biopharmaceutical industry as it represents very delicate and costly procedures. The fundamentals of Protein A-based separation columns used to purify biologics are not fully mastered, as it can be a challenge to elute Protein A-captured biomolecules; *e.g.*, up to 30% can remain trapped in the column after elution [16], causing financial burden on the process.

The Langmuir isotherm was fit to experimental data obtained from QCM frequency shift measurements to derive the equilibrium constants (K_D, K_A), and kinetic rate constants (k_{on}, k_{off}) at varying Enbrel® concentrations. It is shown that while the net binding rate increases with increasing Enbrel® concentration, k_{on} and k_{off} in fact decrease. The decrease in k_{on} and k_{off} can be attributed to mass transport limitations. For the first time, we demonstrate how *in situ* QCM dissipation measurements can be used to provide valuable insights regarding mass transport effects on ligand – receptor interaction kinetics.

2. Materials and methods

2.1. Quartz crystal microbalance (QCM)

The design of the QCM instrument is shown in Fig. 1A. The QCM instrument is housed on a frame composed of chemically resistant type I PVC (McMaster Carr, Cleveland, OH, U.S.A., cat. # 87545K651). The QCM chambers were purchased from Stanford Research Systems (Sunnyvale, CA, U.S.A., cat. # O100RH) and FC-550 flow cells from Inficon (East Syracuse, NY, U.S.A., cat. # 184208). The QCM instrument is computerized using a user interface that was programmed in Labview (National Instruments, v2013). Electronics of the QCM instrument are controlled using a microcontroller unit (Digi-Key, Thief River Falls, MN, U.S.A., cat. # ATMEGA1281-16AURCT-ND). The QCM instrument is integrated to the computer using a USB, type 2 connection (Digi-Key, cat. #MUSBD11130-ND). Power is supplied to the QCM instrument using a 24 V, 180 W AC/DC desktop power supply (Digi-Key, cat. # 1470-1046-ND).

QCM frequency and dissipation measurements are made using a network analyzer (Saunders & Associates, Phoenix, AZ, U.S.A., cat. # 250B). All frequency measurements are acquired using a 10 kHz sweep centered around the 1st, 3rd, and 5th fundamental (*i.e.*, harmonics) frequencies (5 MHz, 15 MHz, and 25 MHz, respectively) of the QCM crystal. The input power is 80 mW. The resulting resonant curves are fit to a Lorentzian function upon which the frequency that had the maximum conductance, f_{max}, was recorded. An algorithm is used to compute the frequency shift and dissipation. A single frequency shift data point is calculated by subtraction the f_{max} at the initial time, t_0, from that of an f_{max} at a later time, t_n of the data acquisition: $f_{max}(t_n) - f_{max}(t_0)$. A single dissipation data point is calculated by computing the half-bandwidth at half-maximum and dividing that value by $f_{max}(t_0)$. The QCM instrument measures both frequency and dissipation simultaneously in real time. Up to 60 measurements can be recorded per minute. When measuring frequency and dissipation from all three harmonics (5 MHz, 15 MHz, 25 MHz) simultaneously using one QCM crystal, it takes 0.1 s to make the three 10 kHz sweeps and record the maximum frequency and calculate the dissipation. Likewise, when using two QCM crystals, it takes 0.2 s to make the six 10 kHz sweeps and record the maximum frequency and calculate the dissipation.

The QCM chambers and flow cells rest inside a stainless steel water reservoir (Fig. 1A). The water reservoir is heated using 4 polyimide flexible heater strips (Omega, Laval, QC, Canada, cat. # KHLV-104/10P). Water reservoir temperature is measured with electronic sensors (Digi-Key, cat. # ADT7310TRZ-REEL7CT-ND). Two sensors are secured to the outside of the water reservoir at opposite ends. The temperature sensors and heating strips are fastened to the stainless steel water reservoir using high-thermal conductivity epoxy (Omega, cat. # OB-101-16). The recordings from each are averaged to yield the temperature measurement. This temperature measurement is fed back into the computer where it is compared to the user set-point. Current through the heater strips is switched on if the measured temperature is below the set-point or switched off if it is above. The water reservoir temperature is displayed on the user interface and on the front of the QCM instrument (Fig. 1A).

Injection of fluids into the QCM chambers is done using syringes. Up to four different syringes can be used for QCM measurements (Fig. 1B). Each syringe is driven using a linear actuator (Electrocraft, Dover, NH, cat. # APPS17). Motion of the linear actuator is controlled using two integrated circuit motor drivers (Digi-Key, cat. # 497-3641-1-ND) and one integrated circuit motor controller (Digi-Key, cat. # 497-2945-5-ND). Flow rates of the electronically-controlled linear actuators are entered through the user interface.

The fluid circuit presented in Fig. 1B was constructed for this experiment. There are a total of two independent QCM chambers, each coupled to two syringes, which are loaded with different fluids. Check-valves (Cole Parmer, Montreal, QC, Canada, cat. # 30505-92) are coupled to the syringes to ensure one-way directional flow. Fluid from each syringe is tied into a chamber using Tygon® tubing (Cole Parmer, cat. # 95666-01) and a Y-connector (Cole Parmer, cat. # 40726-41). Fluids leaving the chambers are collected into Septa-Jar® containers (Fisher Scientific, Ottawa, ON, Canada, cat. # 05-719-313).

2.2. Quartz crystal surface modification

Chromium/gold-plated 5 MHz Maxtek QCM crystals (Inficon, cat. # 149273-1) were modified with functional amine groups using a custom built *n*-heptylamine plasma polymerization (HaPP) reactor [17]. The operating parameters of the HaPP reaction are described elsewhere [18]. Low-fouling carboxymethyl-dextran

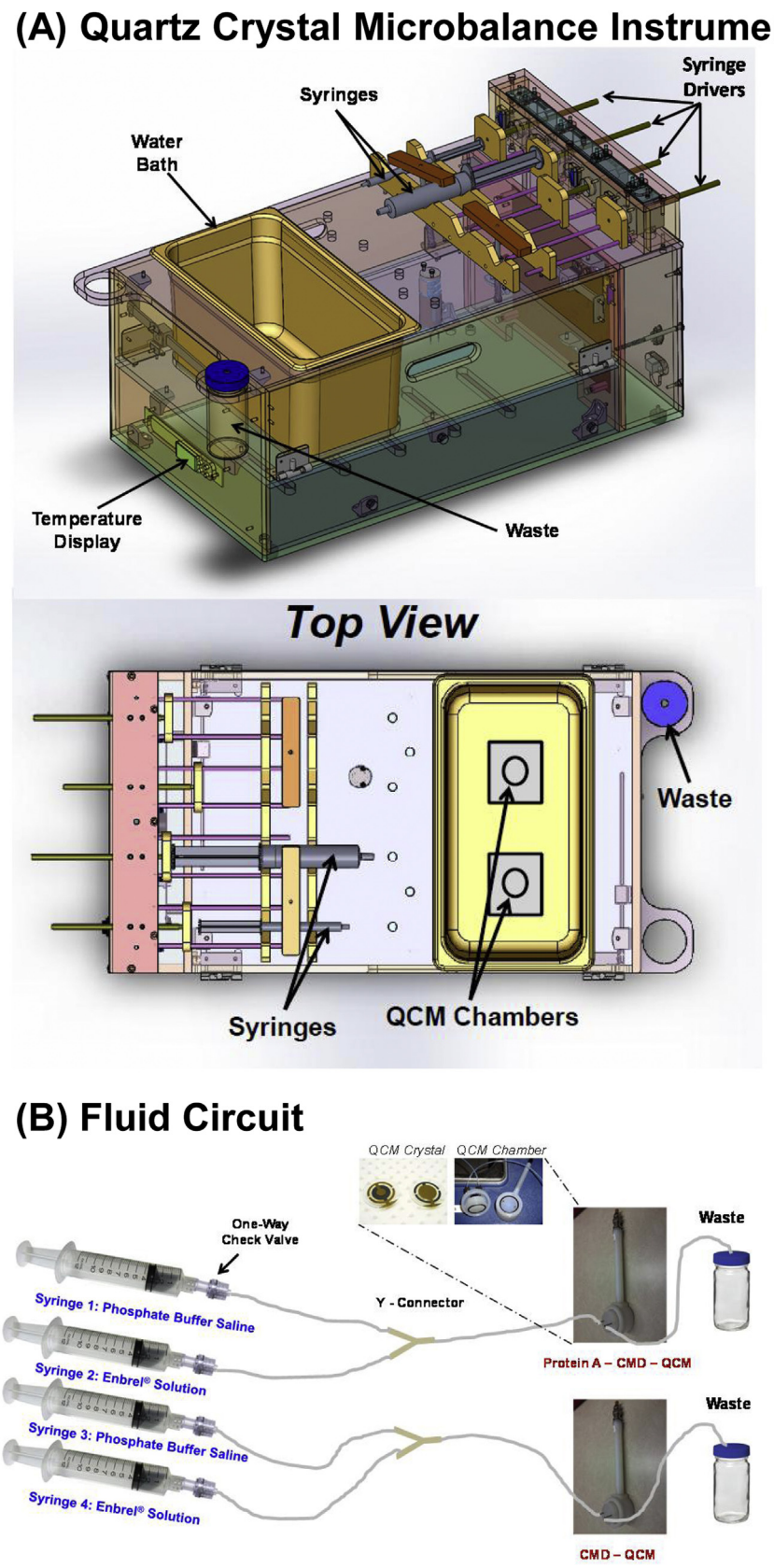

Fig. 1. Schematic of the quartz crystal microbalance (QCM) instrument. (A) The QCM instrument injects fluids into the chambers *via* syringes. The temperature of the QCM chambers is controlled using a water bath. (B) Up to four different solutions can be loaded into syringes and injected into two independent QCM chambers.

(CMD) was covalently grafted to HaPP-modified QCM crystals using carbodiimide chemistry described in detail elsewhere [19]. Recombinant Protein A (Pierce, Rockford, IL, U.S.A., cat. # 21184) was immobilized onto CMD-modified QCM crystals using amine coupling developed in a previous study [20]. Briefly, Protein A was reconstituted in 10 μM $CaCl_2$ aqueous solution to a 0.22 μM (10 μg mL^{-1}) concentration. CMD-modified QCM crystals were activated for 10 min in 200 mM activation solution composed of 1-ethyl-3-(3-dimethylaminopropyl)carbodiimide (EDC, Oakville, ON, Canada, Sigma-Aldrich, cat. # E1769) and N-hydroxysuccinimide (NHS, Sigma-Aldrich, cat. # 130672). Activated surfaces were rinsed in Milli-Q water and then submerged in Protein A solution. The reaction was allowed to proceed for 2 h under gentle agitation. Afterwards, Protein A-modified QCM crystals were rinsed 3 times in phosphate buffered saline (PBS, Fisher Scientific, cat. # BP6651) and stored at 4 °C until use. See Supplementary Tables 1 and 2 for demonstration of the presence of the different thin layers by X-ray photoelectron spectroscopy as well as the functionality of surface-immobilized Protein A by enzyme-linked immunosorbent assay (ELISA).

2.3. Quartz crystal microbalance (QCM) measurements

Protein A- and CMD-modified QCM crystals were placed inside their chambers (Fig. 1B). The crystals were secured inside the chambers using a customized screw-cap torqued to 0.17N m. After crystal installation, chambers were flooded manually with PBS using syringes. The fluid circuit was then installed on the QCM instrument. Prior to QCM measurements, the fluid circuit was equilibrated by running PBS through the chamber for 10 min at a flow rate of 200 μL min^{-1}. Prior to QCM experiments, frequency shift measurements were recorded overnight to ensure a flat baseline was established. All QCM measurements were performed at 23.0 ± 0.1 °C.

QCM experiments consisted of three consecutive injections in which frequency shift and dissipation measurements were continuously recorded. All injections were carried out for 30 min at flow rates of 66 μL min^{-1} which corresponds to a total volume of 2 mL. PBS solution was first injected to ensure a flat baseline was maintained during fluid flow. Immediately after, Enbrel® solution was injected. Enbrel® (Amgen/Pfizer) arrived as a 50 mg mL^{-1} solution. Enbrel® was reconstituted in PBS to concentrations between 0.75–300 ng mL^{-1} (0.005 to 2.0 μM). After Enbrel® solution injections, another PBS injection was performed to close out the experiment.

Frequency shift measurements, ΔF were converted to detected mass, ΔM, using the Sauerbrey equation,

$$\Delta M = -\frac{C_s}{n}\Delta F \tag{1}$$

where C_s, is the manufacturer (Inficon) provided mass sensitivity constant of the QCM crystal, equal to 17.85 ng $(cm^2\ Hz)^{-1}$ and n is the harmonic. In this study, the 1st, 3rd, and 5th harmonics were recorded (n = 1, 3, and 5).

3. Theory and calculations

3.1. Enbrel® - Protein A binding model

Enbrel® is a dimeric fusion protein (MW of 150 kDa) composed of two TNF receptors linked to a sole F_c-portion of an IgG_1 antibody. Protein A is a membrane protein (MW of 42 kDa) containing five high-affinity binding sites that interact with the F_c-portion of most immunoglobulins (including IgG_1). With the Langmuir binding model, the interaction can be written as

$$[L_{Enbrel}] + [R_{ProtA}] \rightleftarrows [LR_{Enbrel-ProtA}] \tag{2}$$

In this study, Protein A is covalently grafted onto a modified QCM crystal surface, thus in Eq. (2), "→" indicates Enbrel® binding "*on*" the Protein A-modified QCM crystal and "⟵" indicates Enbrel® dissociating "*off*" the Protein A-modified QCM crystal.

The net rate of Enbrel® binding to the Protein A-modified QCM crystal is

$$\frac{\partial}{\partial t}[LR_{Enbrel-ProtA}] = \text{Rate On} - \text{Rate Off} \tag{3}$$

$$\frac{\partial}{\partial t}[LR_{Enbrel-ProtA}] = k_{on}[L_{Enbrel}][R_{ProtA}] - k_{off}[LR_{Enbrel-ProtA}] \tag{4}$$

where k_{on} is the association rate constant and k_{off} is the dissociation rate constant. $LR_{Enbrel\text{-}ProtA}$, L_{Enbrel}, and R_{ProtA} are concentrations of the respective species given in molar (M). The units for k_{on} is M^{-1} s^{-1} and for k_{off} is s^{-1}.

The total concentration of Protein A-receptor binding sites, $[R_{ProtA}]_{Total}$, on the modified QCM crystal is

$$[R_{ProtA}]_{Total} = \#\text{Unoccupied Sites} + \#\text{Occupied Sites}$$

$$[R_{ProtA}]_{Total} = [R_{ProtA}] + [LR_{Enbrel-ProtA}] \tag{5}$$

At equilibrium, the net rate is 0 and

$$\text{Rate On} = \text{Rate Off}$$

$$k_{on}[L_{Enbrel}][R_{ProtA}] = k_{off}[LR_{Enbrel-ProtA}] \tag{6}$$

Substitution of Eq. (5) (solved for $[R_{ProtA}]$) into Eq. (6) yields

$$[LR_{Enbrel-ProtA}] = \frac{k_{on}[L_{Enbrel}][R_{ProtA}]_{Total}}{k_{off} + k_{on}[L_{Enbrel}]} \tag{7}$$

Eq. (7) is commonly known as the Langmuir adsorption isotherm. The Langmuir adsorption isotherm quantitatively describes the amount of mass adsorbed onto a surface at a particular concentration.

In QCM measurements, the final frequency change, ΔF_{final}, is directly proportional to the mass attached to the QCM crystal surface. Therefore, $LR_{Enbrel\text{-}ProtA}$ is proportional to ΔF. The maximum frequency change ΔF_{max} occurs when all Protein A sites on the QCM crystal are occupied and thus is proportional to $[R_{ProtA}]_{Total}$. Finally, L_{Enbrel} is proportional to the concentration, $[C]$, of Enbrel® in solution.

Eq. (7) can now be written as

$$\Delta F_{final} = \frac{k_{on}\Delta F_{max}[C]}{k_{off} + k_{on}[C]} \tag{8}$$

Noting that frequency is converted to mass using the Sauerbrey equation (Eq. (1)) and rearranging we get

$$\Delta M_{final} = \frac{\Delta M_{max}[C]}{K_D + [C]} \tag{9}$$

where K_D is the equilibrium dissociation constant given by

$$K_D = \frac{k_{off}}{k_{on}} \tag{10}$$

Note that ΔM_{final} and ΔM_{max} are expressed in units of ng cm^{-2} and K_D and $[C]$ are in units of molar concentration (M).

At non-equilibrium,

$$\frac{\partial}{\partial t}[LR_{Enbrel-ProtA}] \neq 0 \tag{11}$$

Thus, substitution of Eq. (5) (solved for $[R_{ProtA}]$) into Eq. (4) yields,

$$\frac{\partial}{\partial t}[LR_{Enbrel-ProtA}] = k_{on}[L_{Enbrel}]([R_{ProtA}]_{Total} - [LR_{Enbrel-ProtA}]) - k_{off}[LR_{Enbrel-ProtA}] \quad (12)$$

Relating Eq. (12) to QCM measurements as for Eq. (7), we get

$$\frac{\partial \Delta F}{\partial t} = k_{on}[C](\Delta F_{max} - \Delta F) - k_{off}\Delta F \quad (13)$$

Separating Eq. (13) and integrating yields

$$\Delta F = \frac{k_{on}[C]\Delta F_{max}}{k_{on}[C] + k_{off}}(1 - e^{-(k_{on}[C]+k_{off})t}) \quad (14)$$

Noting that frequency is converted to mass using the Sauerbrey equation (Eq. (1)), we get

$$\Delta M = \frac{k_{on}[C]\Delta M_{max}}{k_{on}[C] + k_{off}}(1 - e^{-(k_{on}[C]+k_{off})t}) \quad (15)$$

$$\Delta M = \frac{\Delta M_{max}[C]}{K_D + [C]}(1 - e^{-(k_{on}[C]+k_{off})t}) \quad (16)$$

In this study, Eqs. (9), (10), and (16) are used to calculate k_{on}, k_{off}, and K_D from experimental QCM data. The association constant K_A was calculated using the relation

$$K_A = \frac{1}{K_D} \quad (17)$$

3.2. Calculation of Enbrel®- Protein A kinetic rate and equilibrium binding constants

QCM data were fitted using built-in curve fitting algorithms in OriginPro V8.1. Detected Enbrel® mass, ΔM, as a function of Enbrel® solution concentration, *[C]*, was fitted using the built-in *Extended Langmuir Model (ExtLangmuir1)* algorithm,

$$y = \frac{ax^{g-1}}{1/b + x^{g-1}} \quad (18)$$

Eq. (18) is of the same form as Eq. (9). The coefficient *1/b* yields K_D and substitution of this value into Eq. (17) gives K_A. ΔM as a function of reaction time, *t*, was fitted using the built-in *Box Lucas Model (BoxLucas1)* algorithm

$$y = h\left(1 - e^{-px}\right) \quad (19)$$

Eq. (19) is of the same form as Eq. (16). Applying

$$p = k_{on}[C] + k_{off} \quad (20)$$

While noting that the concentration, *[C]*, is constant (as there is continuous flow of Enbrel® over the course of time, *t*, the QCM measurements are performed) and using the relation of Eq. (10), k_{on} and k_{off} were calculated.

In this study, all kinetic equilibrium (K_A, K_D) and rate constants (k_{on}, k_{off}) were calculated without employing the use of a regeneration solution to analyze dissociation of the ligand from the receptor. Often, the association rate constant k_{on} is calculated using data collected during injection of a sample containing the ligand and the dissociation rate constant k_{off} is calculated using data collected during the injection of a running or regeneration buffer that does not contain the ligand. Therefore, the solution injected during association differs from that during dissociation and thus the k_{off} determined from each of these solutions are not related to the same reaction. In other words, k_{off} during injection of the ligand solution is not the same as during injection of the running/regeneration solution. Thus, when using different solutions during association and dissociation, equilibrium constants K_A and K_D calculated using k_{on} and k_{off} (Eq. (10) and Eq. (17) may not be truly representative of the ligand – receptor interaction under investigation. We did not aim to use a regeneration solution in this study and we believe it is not necessary to use such a solution to analyze dissociation of the ligand (Enbrel®) from the receptor (Protein A).

4. Results and discussion

4.1. Enbrel®- Protein A interaction specificity

To ensure the QCM frequency shifts were a result of specific Enbrel® – Protein A interactions, CMD- and Protein A-CMD-modified QCM crystals were simultaneously compared. The QCM instrument is capable of performing data acquisition simultaneously on two modified QCM crystals (Fig. 1B).

The results are presented in Fig. 2. When Enbrel® comes into contact with a Protein A-modified CMD QCM crystal (Fig. 2A), sensorgrams show a large up shift in detected mass (Fig. 2B), thus confirming Enbrel® capture. In contrast, when there is no Protein A on the CMD-modified QCM crystal (see Fig. 2A), sensorgrams show no mass is detected (see Fig. 2B), thus no Enbrel® capture. Together, these results confirm detected mass in the QCM sensorgrams is due to specific interactions between Enbrel® in solution and Protein A immobilized on CMD-modified QCM crystals. It is important to note that there was no observed loss in detected mass, ΔM, when rinsing with PBS after the Enbrel® injection. Given that ligand – receptor interactions are reversible governed by an equilibrium constant, it is expected that some loss of ΔM should occur. Given that there was no observed loss in ΔM, this indicates that the mass quantity of Enbrel® dissociated from the Protein A-modified CMD-QCM crystal during rinsing with PBS was very low. The mass loss was so low that it was below the detection limit of the QCM instrument and therefore not observable in the QCM sensorgram (see Fig. 2B).

4.2. Enbrel® - Protein A interaction kinetics

Enbrel® – Protein A interactions were modeled using the Langmuir binding model. QCM measurements were performed with Enbrel® solutions at concentrations ranging from 0.75 to 300 ng mL^{-1} (0.005–2 μM). Enbrel® solutions were injected onto Protein A-modified CMD-bearing QCM crystals using the QCM instrument.

A typical QCM sensorgram for each measured concentration is shown in Fig. 3A. Upon Enbrel® solution injection onto Protein A-modified CMD-bearing QCM crystals, there is a clear concentration, *[C]*, dependence on the rate at which detected mass, ΔM, reaches the final maximum, ΔM_{final}. As shown in Fig. 3B, a plot of ΔM_{final} as a function of *[C]* shows that for concentrations lower than 0.1 μM, ΔM_{final} drastically changes. However, at concentrations higher than 0.1 μM, ΔM_{final} changes less drastically. These results imply that as the concentration approaches 0.1 μM and above, nearly all of the available Protein A F_c-binding sites, $[R]_{ProtA}$, are occupied and thus only small additional quantities of Enbrel® can be captured.

Fig. 3B closely resembles the form of the well-established Langmuir adsorption isotherm represented mathematically in Eq. (9). Fitting the curve of Fig. 3B with Eq. (9) yields the equilibrium dissociation constant K_D and from that the corresponding association constant K_A can be calculated using Eq. (17) (Table 1 for values). Fig. 3C closely resembles that of Eq. (16) or more simply written, Eq. (19). Fitting the curve(s) of Fig. 3C yields values for the net binding rate, $k_{on}[C] + k_{off}$ (Table 1 for values). Combining these results with the now known K_D and the relation of Eq. (10), k_{on} and k_{off} can now be calculated for each known concentration, *[C]* (Table 1 for values). Our K_D value of 5.06×10^{-8} M is within the range of those previously reported for Protein A – IgG interactions using SPR [21,22]. Differences in K_D values are likely attributed to the fact that

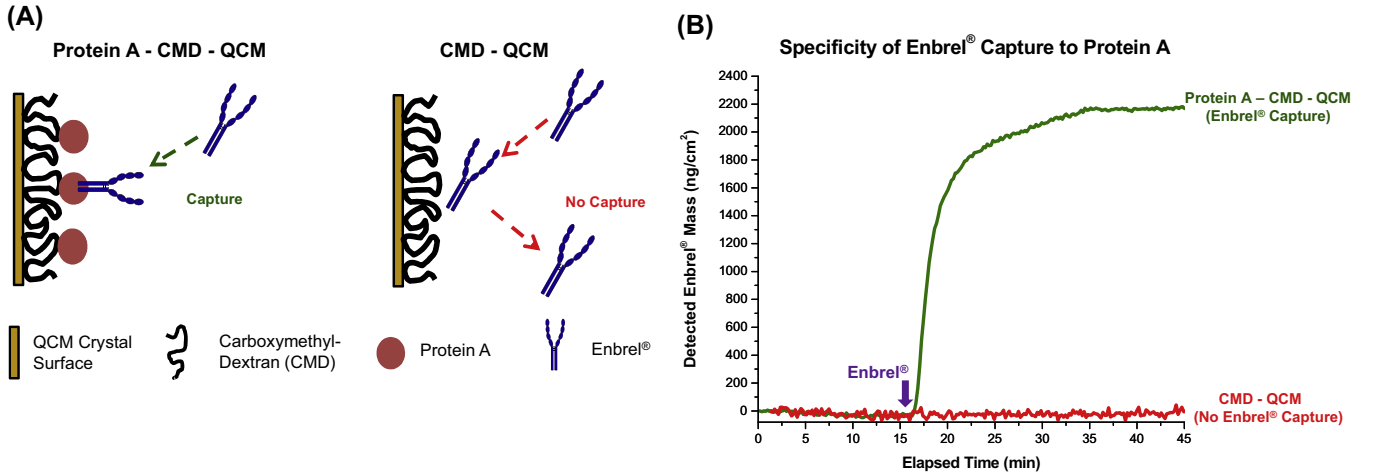

Fig. 2. Enbrel® – Protein A interaction specificity. (A) Pictorial representation of Enbrel® capture with QCM crystals covered with Protein A-modified low-fouling CMD layers *vs.* crystals coated with bare CMD layers. Enbrel® only binds when Protein A is present on the sensor surface. (B) QCM sensorgrams of QCM crystals bearing Protein A-modified CMD layers and those with bare CMD. Mass is only detected when Protein A is present on the sensor surface.

Table 1
Calculated equilibrium constants (K_D, K_A) and kinetic rate constants (k_{on}, k_{off}) of Enbrel® – Protein A interactions.

Equilibrium Dissociation Constant,	$\mathbf{K}_D = 5.06 \times 10^{-8}$ M
Equilibrium Association Constant,	$\mathbf{K}_A = 1.98 \times 10^{7}$ M^{-1}

[C], (μM)	$(\mathbf{k}_{on}\mathbf{[C]} + \mathbf{k}_{off})$, (min^{-1})	$\mathbf{k}_{on}$, (s^{-1} M^{-1})	$\mathbf{k}_{off}$, (s^{-1})
0.005	0.1212	3.634×10^4	1.838×10^{-3}
0.05	0.1274	2.111×10^4	1.068×10^{-3}
0.1	0.1390	1.539×10^4	7.782×10^{-4}
0.2	0.2251	1.497×10^4	7.573×10^{-4}
2	0.3689	2.998×10^3	1.517×10^{-4}
Concentration, ***[C]***		*Association Rate Constant,* $\mathbf{k}_{on}$	
Net Binding Rate, $(\mathbf{k}_{on}\mathbf{[C]} + \mathbf{k}_{off})$		*Dissociation Rate Constant,* $\mathbf{k}_{off}$	

the aforementioned studies employed antibodies and therefore the affinities may vary depending on what F_c-region binds to Protein A.

The goal of real-time label-free biosensor applications, such as those to investigate immunogenicity, is the measurement of antibody concentration [2,3]. The results of Fig. 3 show that if using QCM to analyze antibody concentration, it is necessary to assess both the final detected mass, ΔM_{final}, and the net binding rate, $k_{on}[C] + k_{off}$, depending on concentration. For low concentrations, ΔM_{final} provides the most insight as Fig. 3B shows that adsorbed masses vary noticeably, as was the case for 0.005 and 0.05 μM. There are less noticeable differences in ΔM_{final} for higher concentrations such as 0.1, 0.2, and 2.0 μM. However, as shown in Fig. 3D, at such higher concentrations, $k_{on}[C] + k_{off}$ vary noticeably.

4.3. Mass transport limitations in protein A – Enbrel® interaction kinetics

Interestingly, the results of Table 1 show that k_{on} decreases as $[C]$ increases. While this may appear counterintuitive, this observation can be best explained when considering mass transport limitations. Mass transport limitations influence the association (k_{on}) and dissociation (k_{off}) rate constants. This has been demonstrated previously in a mathematical model showing that mass transport limitation is dependent on the ligand concentration chosen for an experiment [23]. Association is affected *via* diffusion of the ligand (*i.e.*, Enbrel®) to the sensor surface and dissociation *via* re-binding to the sensor surface before there is an opportunity to diffuse away from the sensor surface [24]. The diffusion of a species in a solution is more inhibited as the viscosity of the solvent increases, as stated in the Stokes-Einstein equation.

The more viscous the ligand-containing solution is, the more association/dissociation is affected by mass transport limitations [8]. Biopharmaceutical formulations contain high protein/antibody concentrations along with other additives (*e.g.*, Enbrel® stock solution contains sucrose) and as a result are highly viscous [25]. Therefore, in this study as Enbrel® concentration increases, the solution viscosity also increases (see Supplementary Fig. 1, for an example). The effects of mass transport limitations are best visualized by considering two examples (Fig. 4); the first with a low Enbrel® concentration and the second with a high Enbrel® concentration. The viscosity, μ, of the high Enbrel® concentration (μ_2) solution is higher than that of the low Enbrel® concentration (μ_1). Since $\mu_2 > \mu_1$, the diffusivity, d, is larger for the lower Enbrel® concentration (*i.e.*, $d_1 > d_2$) in accordance with the Stokes-Einstein equation (Fig. 4). As shown in Fig. 4, initially at injection, there is a uniform concentration of Enbrel® at the Protein A-modified biosensor surface and throughout. Because of a rapid initial Enbrel® adsorption, it can be hypothesized that overtime concentration gradients are formed caused by diffusion-limited mass transport. Now Enbrel® transport towards and away from the biosensor surface occurs primarily *via* diffusion. Because $d_1 > d_2$, Enbrel® diffusion at lower concentrations is less affected by mass transport. Therefore, at lower concentrations, Enbrel® diffuses more readily towards and away from the biosensor surface resulting in greater kinetic rate constants with respect to higher Enbrel® concentrations (*i.e.*, $k_{on,1} > k_{on,2}$ and $k_{off,1} > k_{off,2}$). This model is similar to that previously described by O'Shannessy [26] for explaining mass transport limitations of surface plasmon resonance (SPR) for the determination of the kinetic rate (k_{on}, k_{off}) and equilibrium (K_A, K_D) constants.

Mass transport limitations highlighted in Fig. 4 explain the decrease of k_{on} and k_{off} as Enbrel® concentration increases (Table 1). It is also important to explain how the net binding rate, $k_{on}[C] + k_{off}$, increases as Enbrel® concentration increases (Table 1). The rate of rapid adsorption of Enbrel® at initial injection is directly proportional to the concentration, $[C]$. The increase in $[C]$ is large enough that it overcompensates for the decreases in k_{on} and k_{off} to such an extent that the overall net binding rate, $k_{on}[C] + k_{off}$, increases as shown in Table 1.

We believe QCM dissipation measurements, combined with ΔF monitoring, can provide novel insights into mass transport limitations, insights that have yet been exploited using QCM and that are not possible to observe using SPR. In general, QCM dissipation measurements are indicative of the viscoelasticity of the film and the viscosity of the liquid media [13], which in this study corresponds to

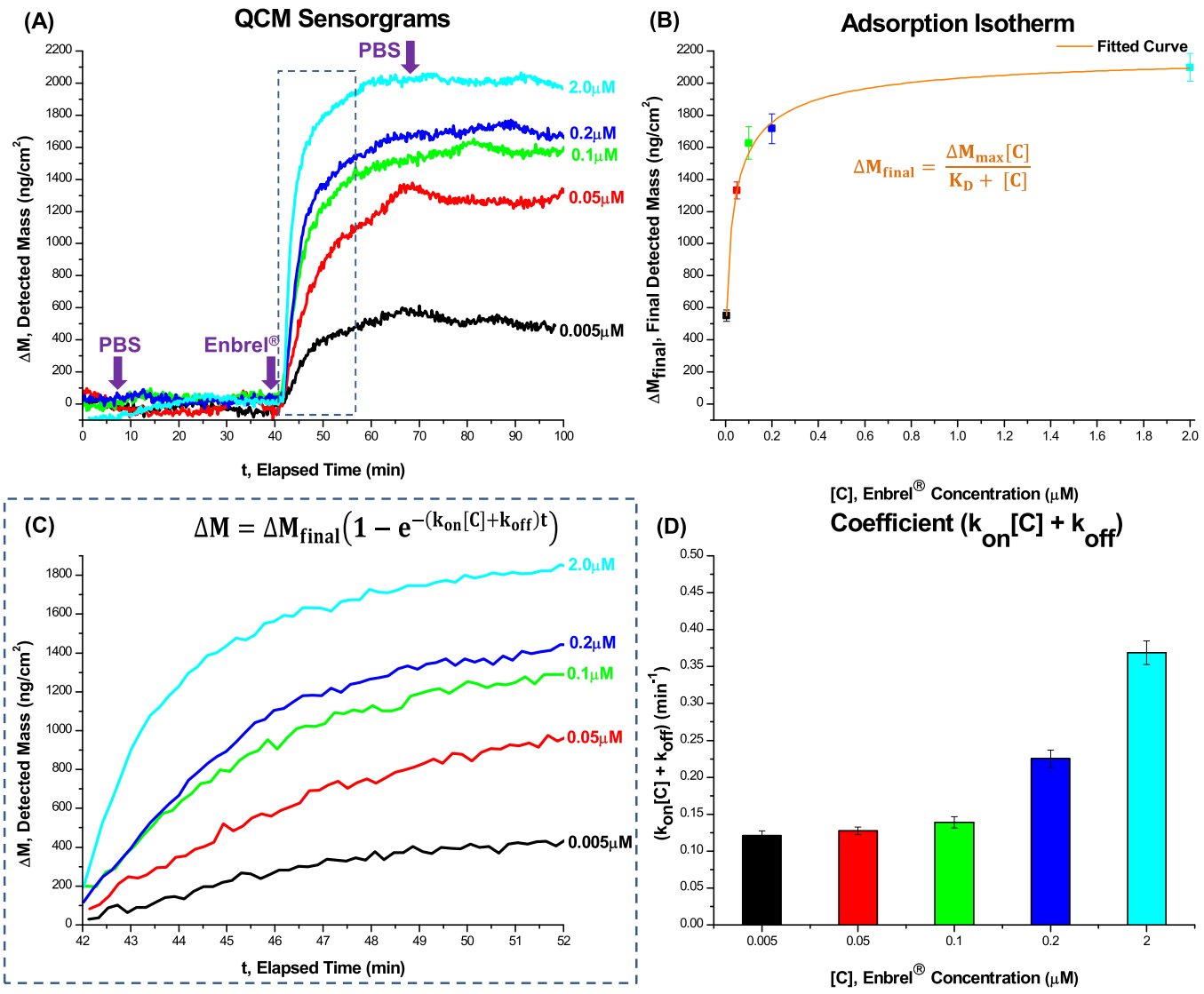

Fig. 3. Quartz crystal microbalance (QCM) results following solution injection at various Enbrel® concentrations over crystals bearing Protein-A modified CMD layers. (A) Representative QCM sensorgrams for each injected Enbrel® concentration. Upon injection of Enbrel®, there is clear up shift in detected mass, ΔM, in a concentration dependent manner. (B) Graph of final detected Enbrel® mass, ΔM_{final}, from the QCM sensorgrams as a function of Enbrel® concentration. The curves take the form of the Langmuir adsorption isotherm given by Eq. (9). Data are presented as the average ± S.E.M. of n = 9 QCM sensorgrams (3 independent injections for each Enbrel® concentration with simultaneous recordings of the 1st, 3rd, and 5th harmonics). (C) Zoom in of QCM sensorgrams during Enbrel® binding to crystals bearing Protein A-modified CMD layers (dashed box). Enbrel® binding takes on the form of Eq. (16). (D) Comparison of the net Enbrel® binding rate, $k_{on}[C] + k_{off}$, at each concentration. Data are represented as the average ± S.E.M. of n = 9 QCM sensorgrams (3 independent injections for each Enbrel® concentration with simultaneous recordings of the 1st, 3rd, and 5th harmonics).

the adsorbed Enbrel® film and the viscosity of the Enbrel® solution, respectively. For bare CMD-modified QCM crystals, because there was no measurable captured Enbrel® (Fig. 2B), changes in ΔD can be attributed mostly to changes in solution viscosity when going from PBS solution to Enbrel® solution or vice versa, as evidenced by Supplementary Fig. 1. For Protein A-modified CMD bearing QCM crystals, the increase in ΔD is a result of both the increase in solution viscosity in going from PBS solution to Enbrel® solution and also the viscoelasticity of the film from Enbrel® capture to the Protein A-modified surface (see Fig. 2B and Supplementary Fig. 1).

As shown in Fig. 5, as Enbrel® concentration increases, ΔD also increases. Although viscoelasticity and solution viscosity are convoluted in ΔD measurements, we hypothesize that the magnitude of solution viscosity relative to that of the layer viscoelasticity can be used to explain the effect of Enbrel® concentration over the observed rate constants. Supplementary Fig. 1 verifies this hypothesis by illustrating the effect of the solution viscosity on the observed overall dissipation changes; here ΔD were monitored after exposing both bare CMD layers and Protein A-bearing CMD layers to two Enbrel® concentrations. Supplementary Fig. 1 reveals that the viscoelasticity of the Enbrel® film remains almost the same as Enbrel® concentration increased from 1.0 μM to 2.0 μM.

Thus, Supplementary Fig. 1 allows us concluding that solutions with higher Enbrel® concentrations are more viscous and hypothesizing Enbrel® diffusion in these solutions is more restricted. These measured changes in ΔD validate the hypothesis that as Enbrel® concentration increases, solution viscosity also increases (supported by Supplementary Fig. 1), causing mass transport to become more limited and thereby reducing diffusion. Enbrel® diffusion towards and away from the biosensor surface would be more limited at higher concentrations, resulting in lower kinetic association (k_{on}) and dissociation (k_{off}) rate constants.

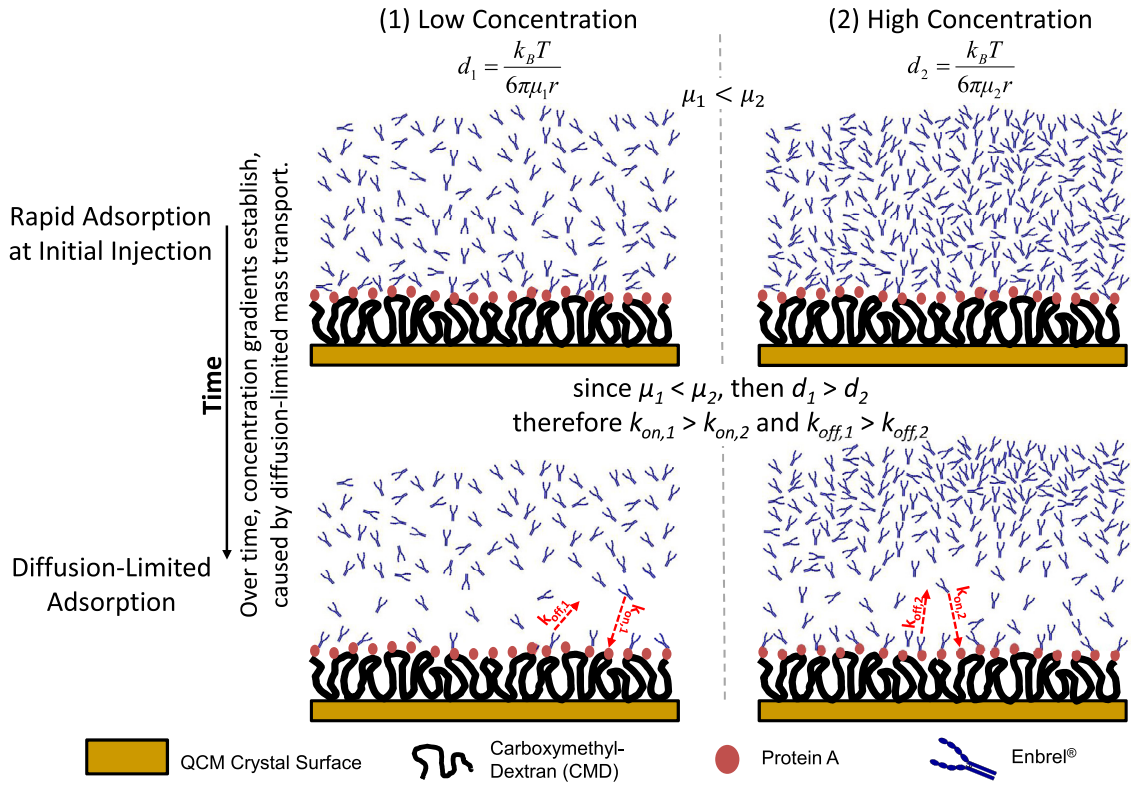

Fig. 4. Pictorial representation of Enbrel® adsorption to Protein A-modified CMD bearing QCM crystals at low and high concentrations. Higher Enbrel® solution concentrations have higher viscosities, μ, than those of lower concentration ($\mu_1 < \mu_2$). Therefore, according to the Stokes-Einstein equation, the diffusivity, d, in solutions with lower concentration is larger than that in solutions of higher concentrations ($d_1 > d_2$). At initial injection, there is a uniform concentration of Enbrel® throughout. Upon rapid adsorption, concentration gradients establish caused by diffusion-limited mass transport. Because diffusion is more limited at high concentrations ($d_1 > d_2$), Enbrel® transports at a slower rate towards the biosensor surface resulting in a lower kinetic on-rate constant, $k_{on,2}$, in comparison to that ($k_{on,1}$) at a lower concentration. Similarly, at high concentrations, Enbrel® transports slower away from the biosensor surface resulting in a lower kinetic off-rate constant $k_{off,2}$ in comparison to that ($k_{off,1}$) at a lower concentration. In summary, since $\mu_1 < \mu_2$, then $d_1 > d_2$ according to the Stokes-Einstein equation, therefore $k_{on,1} > k_{on,2}$ and $k_{off,1} > k_{off,2}$.

5. Conclusions

The present study suggests that quartz crystal microbalance (QCM) is a good potential real-time label-free biosensor platform for the biopharmaceutical industry. Results demonstrate QCM is capable of assessing the kinetics of ligand – receptor interactions, as was done for Protein A – Etanercept. The QCM data can also provide insight regarding antibody concentration of the solution under investigation. Specifically, ΔM_{final} (for lower concentrations) and $k_{on}[C] + k_{off}$ (for higher concentrations), give quantitative insights on antibody concentration. For instance, it is important to know concentration for monitoring the efficiency of antibody-producing cell lines during bioprocess development [7]. QCM could thus also be used just like SPR in the past to analyze protein/antibody concentrations in crude supernatant samples from bioreactor cultures to determine if a cell line is efficiently producing the desired protein/antibody [5,6,27]. Depending on the levels of produced protein/antibody, one could for example, optimize cell culture parameters or reconsider the choice of cell line to accelerate and improve bioprocess development. Finally, it is worthwhile to discuss potential applications QCM has in the development of bioseparation processes. Bioseparation is recognized as a major bottleneck in antibody production [4]. Protein A affinity chromatography is a commonly used antibody purification process [28]. After Protein A capture of the antibody in the purification process, it is necessary to recover the captured antibody in a subsequent step. QCM could be used to evaluate and optimize solutions for antibody elution, similarly to how it has been suggested SPR be employed for antibody purification process development [7]. Using QCM, elution solution characteristics (*e.g.*, pH, ionic strength, *etc.*) and operating parameters (*e.g.*, temperature, flowrate, *etc.*) could be screened to determine the mildest conditions necessary to improve the dissociation of the antibody from Protein A. Potential elution solutions could be assessed quantitatively comparing their dissociation rate constants (k_{off}).

The QCM analysis platform and Langmuir binding model are not without their disadvantages and limitations. An intrinsic drawback of QCM is that frequency measurements, and by extension the detected mass, are effected by temperature variations. If temperature increases, frequency decreases and vice versa. QCM frequency measurements are so sensitive to temperature that even when the temperature is controlled to ±0.1 °C, as was done in this study, small oscillations can still be observed before and after Enbrel® injection (Fig. 3A). Another drawback of QCM is that the Sauerbrey equation (Eq. (1)) assumes the added mass layer is completely rigid and uniformly distributed throughout the sensor surface [29]. A large therapeutic biologic such as Enbrel® is not completely rigid nor is a Protein A-modified CMD bearing QCM crystal surface. With non-rigid adlayer(s) on the QCM sensor surface, the Sauerbrey equation underestimates the detected mass, ΔM [30]. The Langmuir binding model makes assumptions that do not necessarily hold true. The model assumes that the biosensor surface is completely two-dimensional and all binding sites are equally active. This assumption is not true as Protein A adds additional surface roughness. Langmuir binding also assumes that there is no interaction between adsorbed molecules which is unlikely the case when the adsorbate is a large molecule such as Enbrel®.

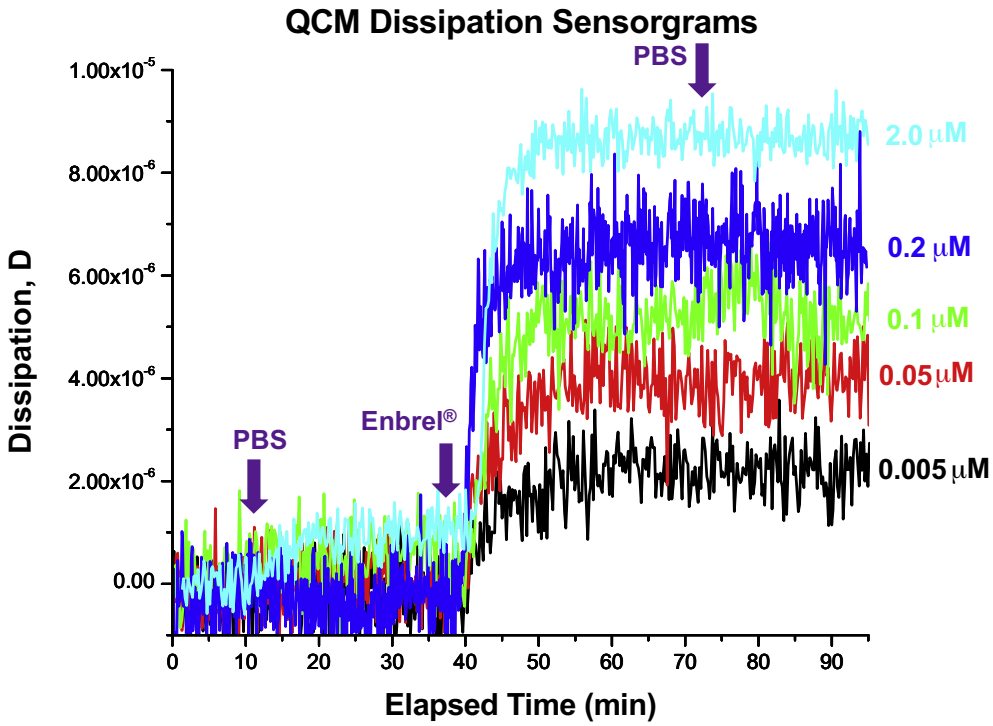

Concentration, [C] (μM)	Change in Dissipation, ΔD
0.005	(1.784 ± 0.034) x 10^{-6}
0.05	(3.875 ± 0.014) x 10^{-6}
0.1	(4.787 ± 0.100) x 10^{-6}
0.2	(6.416 ± 0.089) x 10^{-6}
2	(8.752 ± 0.521) x 10^{-6}

Fig. 5. Representative quartz crystal microbalance (QCM) sensorgrams of dissipation measurements. QCM sensorgrams show the increase in dissipation, ΔD, as Enbrel® concentration increases. This indicates that solution viscosity increases with increased Enbrel® concentration and mass transport limitations thus become more impactful on the kinetic rate constants k_{on} and k_{off}. ΔD data are presented as the average ± S.E.M (n = 3). Supplemental Fig. 1 reveals that ΔD associated with the Enbrel® solution viscosity increased while that corresponding to the viscoelasticity of the Enbrel® film remains almost the same, as Enbrel® concentration increased from 1.0 μM to 2.0 μM.

The QCM provides insights on the effects of mass transport limitations on kinetic data in an *in situ* manner given it a distinct advantage over SPR. This is done through dissipation measurements on receptor-bearing surfaces (here Protein A –CMD-covered QCM crystals) in parallel with a low-fouling layer (here bare CMD-covered QCM crystals) to deconvolute information on the viscosity of the solution undergoing analysis from the viscoelasticity of the film. This could allow, for example, investigating the possible effects of solution viscosity on binding kinetics of different biologics. Dissipation measurements are not possible with the widely used method of SPR. Despite the drawbacks, together each of the aforementioned results supports the use of the QCM instrument and methods developed here as an alternative or complimentary real-time label-free biosensor analysis platform.

Acknowledgements

The authors are grateful to the Québec Consortium for Drug Discovery (CQDM, *Consortium québécois sur la découverte du médicament*) for their financial support of this work, to Serge Gagnon and Marc Couture for their assistance in the construction of the QCM instrument, and to Dr. Tamás Fülöp for providing the Enbrel®.

Appendix A. Supplementary data

Supplementary data associated with this article can be found, in the online version, at http://dx.doi.org/10.1016/j.colsurfb.2016.10.036.

References

[1] Z. Kaymakcalan, P. Sakorafas, S. Bose, S. Scesney, L. Xiong, D.K. Hanzatian, J. Salfeld, E.H. Sasso, Clin. Immunol. 131 (2009) 308.
[2] D.T. Mytych, S. La, T. Barger, J. Ferbas, S.J. Swanson, J. Pharm. Biomed. Anal. 49 (2009) 415.
[3] K. Stubenrauch, U. Wessels, R. Vogel, J. Schleypen, Anal. Biochem. 390 (2009) 189.
[4] M. Arnold, H. Bittermann, B. Kalbfuss-Zimmermann, T. Neumann, K. Schmidt, R. Sekul, F. Hilbrig, H. Ludolph, R. Freitag, J. Chromatogr. A 1218 (2011) 4649.
[5] R. Jacquemart, N. Chavane, Y. Durocher, C. Hoemann, G. De Crescenzo, M. Jolicoeur, Biotechnol. Bioeng. 100 (2008) 184.
[6] G. Stybayeva, M. Kairova, E. Ramanculov, A.L. Simonian, A. Revzin, Colloids Surf. B 80 (2010) 251.
[7] P. Thillaivinayagalingam, J. Gommeaux, M. McLoughlin, D. Collins, A.R. Newcombe, J. Chromatogr. B 878 (2010) 149.
[8] N.J. de Mol, E. Plomp, M.J.E. Fischer, R. Ruijtenbeek, Anal. Biochem. 279 (2000) 61.
[9] L.E. Agafonova, V.V. Shumyantseva, A.I. Archakov, Chem. Phys. Lett. 604 (2014) 5.
[10] X. Li, S. Song, Q. Shuai, Y. Pei, T. Aastrup, Y. Pei, Z. Pei, Sci. Rep. 5 (2015) 14066.
[11] Y. Liu, W. Zhang, X. Yu, H. Zhang, R. Zhao, D. Shangguan, Y. Li, B. Shen, G. Liu, Sens. Actuators B 99 (2004) 416.

[12] H. Ogi, K. Motohisa, K. Hatanaka, T. Ohmori, M. Hirao, M. Nishiyama, Biosens. Bioelectron. 22 (2007) 3238.
[13] D. Johannsmann, Phys. Chem. Chem. Phys. 10 (2008) 4516.
[14] S. Ghose, J. Zhang, L. Conley, R. Caple, K.P. Williams, D. Cecchini, Biotechnol. Prog. 30 (2014) 1335.
[15] D. Tracey, L. Klareskog, E.H. Sasso, J.G. Salfeld, P.P. Tak, Pharmacol. Ther. 117 (2008) 244.
[16] S. Chollangi, R. Parker, N. Singh, Y. Li, M. Borys, Z. Li, Biotechnol. Bioeng. 112 (2015) 2292.
[17] Y. Martin, D. Boutin, P. Vermette, Thin Solid Films 515 (2007) 6844.
[18] E.A. Dubiel, C. Kuehn, R. Wang, P. Vermette, Colloids Surf. B 89 (2012) 117.
[19] E. Monchaux, P. Vermette, Biomacromolecules 8 (2007) 3668.
[20] E.A. Dubiel, P. Vermette, Colloids Surf. B 95 (2012) 266.
[21] N. Islam, F. Shen, P.V. Gurgel, O.J. Rojas, R.G. Carbonell, Biosens. Bioelectron. 58 (2014) 380.
[22] Z. Wang, Z. Cheng, V. Singh, Z. Zheng, Y. Wang, S. Li, L. Song, J. Zhu, Anal. Chem. 86 (2014) 1430.
[23] P. Schuck, A.P. Minton, Anal. Biochem. 240 (1996) 262.
[24] P. Schuck, H. Zhao, Methods Mol. Biol. 627 (2010) 15.
[25] A.R. Patel, B.A. Kerwin, S.R. Kanapuram, J. Pharm. Sci. 98 (2009) 3108.
[26] D.J. O'Shannessy, Curr. Opin. Biotechnol. 5 (1994) 65.
[27] A.R. Newcombe, C. Cresswell, S. Davies, F. Pearce, K. O'Donovan, R. Francis, Process Biochem. 41 (2006) 842.
[28] S. Flatman, I. Alam, J. Gerard, N. Mussa, J. Chromatogr. B 848 (2007) 79.
[29] Y. Luan, D. Li, Y. Wang, X. Liu, J.L. Brash, H. Chen, Langmuir 30 (2014) 1029.
[30] M.V. Voinova, M. Jonson, B. Kasemo, Biosens. Bioelectron. 17 (2002) 835.